A proof-of-concept study in small and large animal models for coupling liver normothermic machine perfusion with mesenchymal stromal cell bioreactors

Umberto Cillo[1,10], Caterina Lonati [2,10] ✉, Alessandra Bertacco[1], Lucrezia Magnini[2], Michele Battistin [2], Liver NMP Consortium*, Lara Borsetto[1], Francesco Dazzi[3], David Al-Adra[4], Enrico Gringeri[1], Maria Laura Bacci [5], Andrea Schlegel[2,6] & Daniele Dondossola[7,8]

To fully harness mesenchymal-stromal-cells (MSCs)' benefits during Normothermic Machine Perfusion (NMP), we developed an advanced NMP platform coupled with a MSC-bioreactor and investigated its bio-molecular effects and clinical feasibility using rat and porcine models. The study involved three work packages: 1) Development ($n = 5$): MSC-bioreactors were subjected to 4 h-liverless perfusion; 2) Rat model ($n = 10$): livers were perfused for 4 h on the MSC-bioreactor-circuit or with the standard platform; 3) Porcine model ($n = 6$): livers were perfused using a clinical device integrated with a MSC-bioreactor or in its standard setup. MSCs showed intact stem-core properties after liverless-NMP. Liver NMP induced specific, liver-tailored, changes in MSCs' secretome. Rat livers exposed to bioreactor-based perfusion produced more bile, released less damage and pro-inflammatory biomarkers, and showed improved mithocondrial function than those subjected to standard NMP. MSC-bioreactor integration into a clinical device resulted in no machine failure and perfusion-related injury. This proof-of-concept study presents a novel MSC-based liver NMP platform that could reduce the deleterious effects of ischemia/reperfusion before transplantation.

Normothermic machine perfusion (NMP) holds the potential to serve as an ideal platform for ex situ improvement of liver quality. While offering the potential to increase the number of livers suitable for transplantation[1], the procedure provides only partial benefits on transplantation outcome[2]. Although different protective pathways are induced during perfusion at physiological temperature[3,4], these endogenous mechanisms cannot fully prevent the deleterious consequences elicited by peri-mortem events[5–7] and ischemia/reperfusion (IR)[8,9], especially in extended criteria donors (ECD) livers[10–13].

Moreover, the restoration of normothermia impacts liver homeostasis from the onset of perfusion, thereby limiting the overall efficacy of NMP[14–16]. The application of supplementary interventions emerges, therefore, as a logical and interesting concept to unlock the full potential of NMP.

Mesenchymal stromal cells (MSCs) could represent effective therapeutic agents for mitigating the damage induced immediately after reperfusion[17–21]. In fact, such stem cells proved to effectively reduce hepatic IRI in vivo[22,23] and to exert multiple beneficial effects

when administered during experimental liver MP[24–29]. Moreover, ex situ treatment with MSCs was associated with improved histopathological scores and longer survival times after liver transplantation[24,29].

Despite these promising results, the current strategy for ex situ delivery of cell-based therapies has limitations that hamper the full realization of MSCs' therapeutic effects during NMP[17]. In fact, exposure of thawed MSCs to the perfusion fluid was associated with reduced cell viability and generation of reactive oxygen species (ROS)[30]. Furthermore, non-adherent culture condition, as required during NMP, causes the activation of apoptosis programs in these cells[30,31]. Cryopreservation itself reduces stem cell survival and trigger oxidative stress[30]. Finally, cell administration into the organ microvasculature and their subsequent migration to the graft tissue still raise important concerns related to the risk of microvascular embolism[32,33] and accidental differentiation of MSCs[34].

Therefore, we aimed to develop an advanced perfusion platform to harness the potentials of MSCs during NMP, while avoiding any unwanted effects related to their direct supplementation to the perfusate. The design of the novel circuit was guided by the basic mechanisms underlying stem cell biology. First, while MSCs-induced protection was initially attributed to their ability to replace damaged cells, it is now established that most of the stem cell-related benefits depend on the release of multiple soluble factors[21,35] and extracellular vesicles (EVs)[35]. Second, MSCs secretory activity is boosted after exposure to inflammatory microenvironments, and different inflammatory stimuli can elicit distinct responses[36], a process referred to as cell licensing[37–39].

Based on these observations and on the expertise acquired from the use of MSCs-derived EVs during ex vivo lung perfusion[40], we elected to seed fresh MSCs into hollow fiber bioreactors and to incorporate them into our well-established circuit for rat liver NMP[41,42]. An initial work package (WP) investigated feasibility and suitability of this novel configuration by assessing MSC viability, secretory activity, and immunophenotype after cell exposure to a perfusion procedure performed in the absence of the liver. In a subsequent research phase, rat liver NMP experiments were carried out to investigate the effects exerted by the bioreactor-based perfusion on hepatic function, energetics, and inflammatory status. Finally, the knowledge acquired during the small animal study was translated into a large animal model to explore the feasibility of MSC-bioreactor integration into a perfusion device suitable for human use.

Results
Study design
The present research was designed according to the "Planning Research and Experimental Procedures on Animals: Recommendations for Excellence" (PREPARE) guidelines[43] and comprises three sequential WPs.

1. Development of the advanced NMP platform coupled with a MSC-bioreactor. The bioreactors (Aferetica srl, Bologna, Italy; Supplementary Fig. 1) were prepared by the research team of the University of Padua (Padua lab) using human adipose tissue-derived MSCs. Then, MSC-bioreactors were shipped to the Fondazione Ca' Granda Ospedale Maggiore Policlinico, Milan (Milan lab). After overnight resting, the bioreactors were connected to the perfusion system and liverless NMP experiments (n = 5) were carried out to test the functionality and stability of the novel circuit configuration. In addition, we investigated whether the perfusion procedure itself modulates MSCs viability and immunophenotype.

2. Bioreactor-based liver NMP in a rat model. This WP investigated the MSC-derived secretome and its effects on the liver during NMP (Supplementary Table 1). As demonstrated in the in vitro study (WP1), MSC-bioreactors were prepared in the Padua Lab and then shipped to the Milan Lab, where they were integrated into an established NMP circuit for small animals[41,42,44]. The novel platform was used to perfuse rat livers (NMP+bioreactor, n = 5) for 4 h. The results provided by these experiments were compared with those obtained from standard liver NMP (NMP, n = 5). Isolated livers exposed to static cold storage (SCS) alone were likewise included in the bio-molecular investigations (SCS, n = 5), while liver biopsies obtained from animal in resting conditions were used as reference controls (Native, n = 5).

3. Bioreactor-based liver NMP in a large animal model. To investigate the technical feasibility of integrating MSC-bioreactors into a NMP device for clinical use, we performed a pilot study using porcine livers. Briefly, bioreactors were prepared following the same procedure described for the small animal study, but using human plasmafilters (Aferetica srl). The bioreactors were then connected to the Liver Assist® device (XVIVO Perfusion AB, Sweden). Next, to test whether the novel configuration could sustain the protocol for clinical NMP, livers procured from porcine donors were subjected to NMP with the MSC-bioreactor (NMP+bioreactor, n = 3) or without it (NMP, n = 3).

Development of the advanced platform for rat liver NMP coupled with the MSC-bioreactor
Assessment of MSC viability after bioreactor shipment. Upon delivery of the bioreactor to the Milan lab, supernatants were collected and analyzed to detect any signs of cell stress or death. Glucose and lactate concentrations were significantly different compared to the reference value of the culturing medium (Supplementary Table 2), indicating that MSCs consumed glucose and produced lactate during shipment. There was a negligibile release of the apoptotic marker caspase-cleaved keratin 18 (CK18) (1.46 ± 0.02 UI). Conversely, a sizable amount of 8-hydroxy-2'-deoxyguanosine (8-OHdG) was observed in the supernatants (28211 ± 1489 pg). A total of $5 \times 10^4 \pm 0.1 \times 10^4$ detached cells were detected in the supernatants, corresponding to 0.25% of the number of cells originally seeded in the bioreactor.

MSC-bioreactor integration into the perfusion system. Figure 1 schematizes the set-up of the novel perfusion system coupled with the MSC-bioreactor (Supplementary Fig. 1). The bioreactor is included in a closed parallel circuit equipped with a dedicated roller pump. A stopcock for perfusate collection is placed downstream the bioreactor and before the liver chamber (Fig. 1).

**Liverless NMP using the NMP platform equipped with the MSC-bioreactor and MSCs characterization at the end of the procedure.** No circulating cells, spontaneously detached from the bioreactor, were detected in the perfusate samples collected throughout liverless-NMP.

Decreased glucose and increased lactate concentrations were observed over the procedure (p = 0.085 and p > 0.0001, respectively; Fig. 2a), while perfusate CK18 levels remained stable (p = 0.682, Fig. 2b). On the other hand, perfusate samples showed increasing concentrations of cytokines Interleukin (IL)-8 and IL-1ra (p = 0.018 and p = 0.002, respectively; Fig. 2c). Of interest, while no expression of IDO was revelaed in the bioreactor supernatants, this molecule was induced during the liverless perfusion procedure (from 190.40 ± 39.11 at 1 h to 115.55 ± 13.73 ng at 4 h). A sustained release of the oxidative stress marker 8-OHdG was likewise observed (from 17193 ± 2211 pg at 1 h to 189375 ± 3532 pg at 4 h, p = 0.730).

Analysis of the EVs indicated that $7.56 \times 10^{10} \pm 1.96 \times 10^{10}$ particles with an average size of 145.92 ± 7.20 nm were released in the perfusate.

Bioreactor transmembrane pressure throughout the liverless perfusion procedure and perfusate gas-analysis are reported in Supplementary Figs. 2 and 3, respectively.

Cells harvested at the end of NMP had 98% viability and when cultured in vitro exhibited the specific features of MSCs, with spindle-
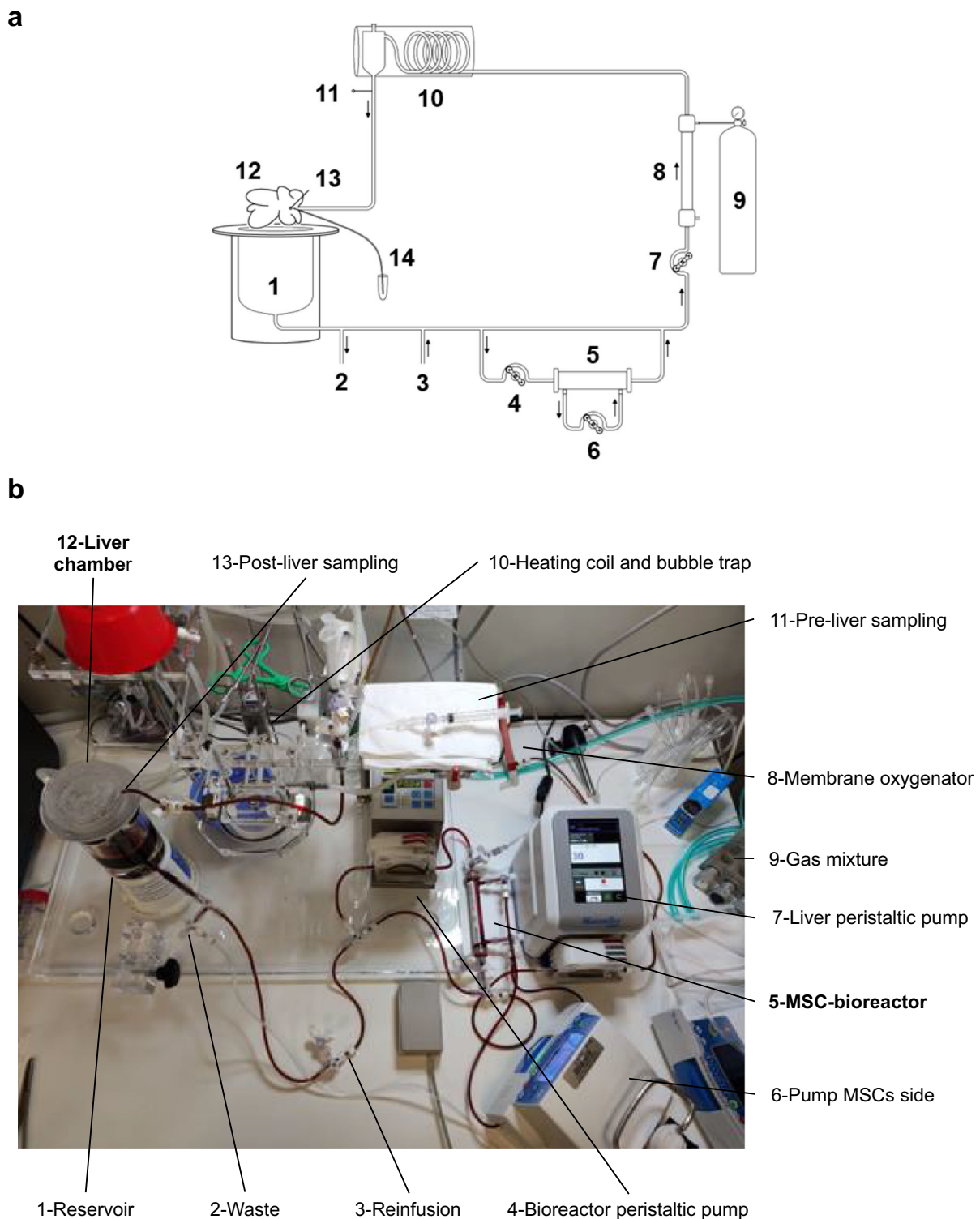
Fig. 1 | Set up of the NMP platform coupled with the MSC-bioreactor.
a Schematic diagram and **b** Picture of the NMP platform for small animal models coupled with the MSC-bioreactor. The bioreactor is perfused in a closed parallel circuit that includes a dedicated roller pump. A stopcocks for perfusion fluid collection is placed downstream the MSC-bioreactor and upstream the liver chamber.

1, Reservoir; 2, Waste; 3, Reinfusion; 4, Bioreactor peristaltic pump; 5, Bioreactor; 6, Pump MSCs side; 7, Liver peristaltic pump; 8, Membrane oxygenator; 9, Gas mixture; 10, Heating coil and bubble trap; 11, Pre-liver sampling; 12, Liver; 13, Post-liver sampling; 14; Bile collection. Abbreviations: MSCs mesenchymal stromal cells.

shaped morphology, abundant production of extracellular matrix, and high colony formation rate (Fig. 2d).

Flow cytometry revealed a preserved expression of MSC-specific markers CD29, CD73, CD90, CD105, whereas the hematological markers CD31, CD34, and CD45 were not measurable (Fig. 2e).

Bioreactor-based liver NMP in a rat model
Analysis of the MSC-derived paracrine factors and EVs released during liver NMP. The comparison between perfusate samples collected during liverless NMP and those of the liver NMP+bioreactor group revealed substantial differences in several of the factors
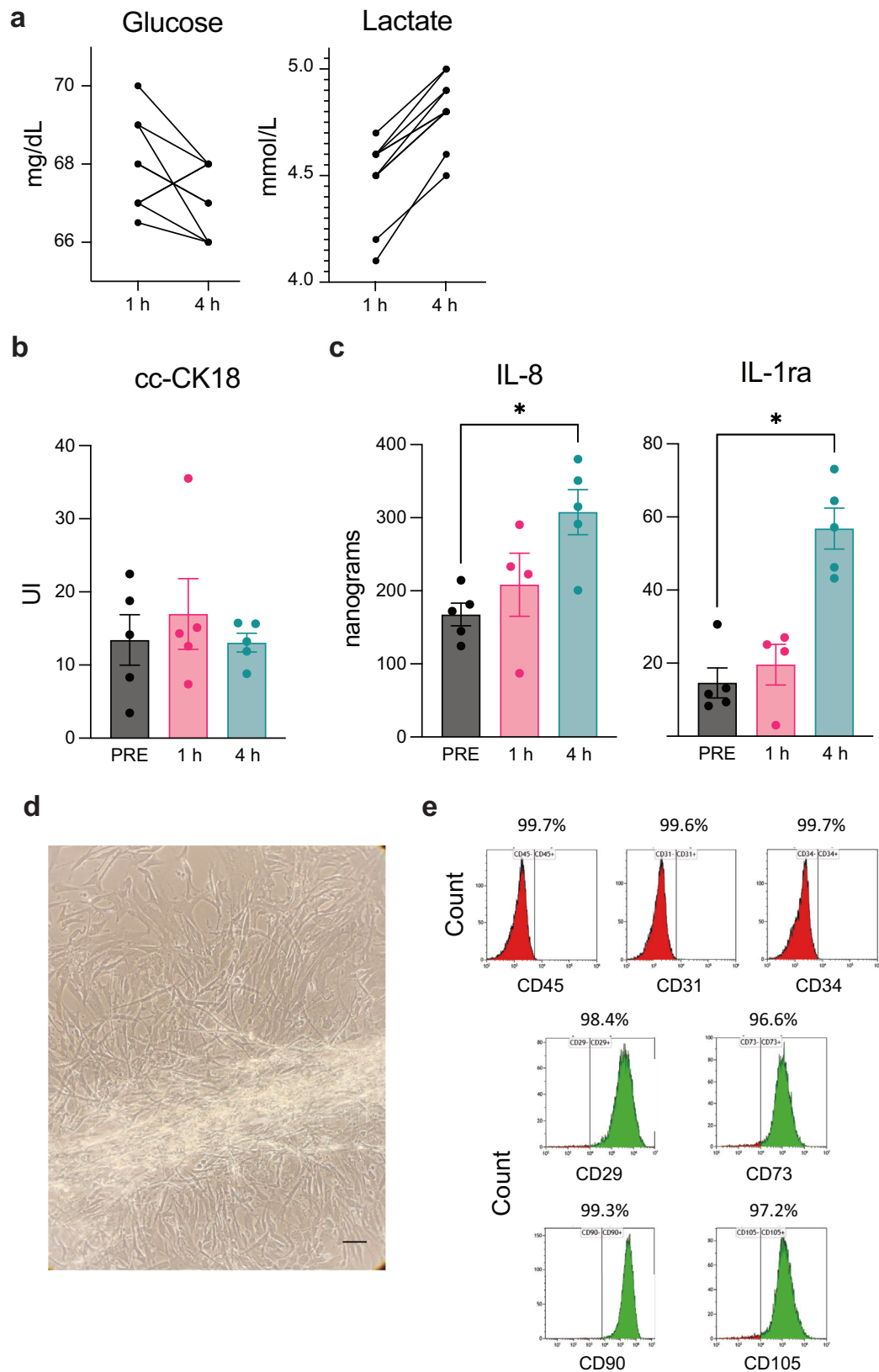
released by MSCs (Fig. 3a). More specifically, among the molecules whose expression increased following MSCs' exposure to the liver-derived soluble factors, there were mediators with prominent anti-inflammatory properties, such as IL-10 (FDR-adjusted p-value for the comparison liverless NMP vs liver NMP+bioreactor: $p = 0.002$)

and IL-1ra ($p = 0.017$). Of interest, the protective mediator IL-4 was secreted by MSCs exclusively in the context of liver NMP. Higher amounts of Galectin-3 (p-value of interaction: $p = 0.002$) and IL-18 ($p = 0.002$) were likewise detected in this setting. In contrast, IDO ($p = 0.024$), IL-6 ($p < 0.001$), and IL-8 ($p = 0.002$)

Fig. 2 | MSCs remained metabolically active during liverless NMP and showed preserved stemness-specific characteristics at the end of the procedure. a Perfusate gas analysis indicated glucose consumption and lactate production during liverless NMP. Estimation plots illustrate *n* = 5 liverless NMP experiments, with two measurements taken for each procedure (i.e., upstream and downstream of the MSCs-bioreactor). One-sided paired t-test, *p*-value: Glucose *p* = 0.085; Lactate: *p* < 0.0001. **b** The release of the apoptotic marker CK18 was stable over liverless NMP. Bars illustrate mean ± SEM, *n* = 5 biologically independent replicates. PRE denotes the supernatants immediately before bioreactors connection to the NMP circuit. One-way RM ANOVA, *p* = 0.682. **c** The MSCs seeded in the bioreactor secreted increasing amounts of IL-8 and IL-1ra during the liverless procedure. Bars illustrate mean ± SEM, *n* = 5 biologically independent replicates. PRE denotes the supernatants immediately before bioreactors connection to the NMP circuit. One-

way ANOVA, *p*-value vs PRE: IL-8 *p* = 0.018; IL-1ra *p* = 0.002. Asterisks denote *p < 0.05. MSCs were harvested from the bioreactor at the end of liverless NMP and cultured in vitro under standard conditions until reaching 90% confluence. **d** Bioreactor-detached MSCs' cultures displayed a spindle-shaped morphology and abundant production of extracellular matrix, which are well-recognized morphological characteristics of stem cells. A representative image captured at 40x magnification is shown; the bar scale on the bottom right denotes 100 micron. **e** After 9 ± 3 days of in vitro culturing, cells were enzymatically harvested for FACs analysis, which revealed a preserved expression of a set of MSC-specific markers (CD29, CD73, CD90, CD105). In contrast, the hematopoietic stem cell markers CD45, CD31, and CD34 were not detected. Five independent replicates were analyzed for each experimental condition. Abbreviations: cc-CK18, caspase-cleaved cytokeratin 18; IL-6, Interleukin 6; IL-1ra, Interleukin 1 receptor antagonist.

Human mediators

	Liver	1h	2h	3h	4h	p-value
ANGPTL4	-	11066	6692	10878	13524	**0.024int**
	+	7596	12826	12506	10971	
CCL2	-	2107	2187	2106	2096	0.570
	+	2409	2221	1992	2315	
Galectin-3	-	2395	2784	3265	4301	**0.002int**
	+	4656	5443	6079	5853	
Galectin-9	-	17857	15217	11373	9858	0.858
	+	13106	22689	18663	11850	
IDO	-	190399	175677	136151	115552	**0.024**
	+	99608	86240	96943	126931	
IL-1ra	-	2425	3224	2778	3704	**0.017**
	+	3669	4512	4109	5721	
IL-4	-					**NA**
	+	667	499	532	321	
IL-6	-	10612	11629	11573	12083	**<0.001**
	+	4489	3460	2419	2113	
IL-8	-	51315	52728	55468	66240	**0.002**
	+	22808	23927	23897	19622	
IL-10	-	493	532	378	562	**0.002**
	+	1101	817	1025	676	
IL-13	-	5010	5085	4359	4188	**0.009int**
	+	4611	4520	4421	4591	
IL-18	-	24	32	12	57	0.080
	+	32	138	65	52	
IL-33	-	86	119	104	116	**0.013**
	+	115	185	163	161	

MIN				MAX
12	782	4330	11908	190399

Total release, pg

Fig. 3 | Changes in the MSC secretome after exposure to the rat liver-derived soluble factors during NMP. a The concentration of selected MSC-related effectors was significantly different in the perfusates collected throughout liverless NMP compared with those withdrawn during liver NMP+bioreactor. Five independent replicates were analyzed for each experimental condition. Two-way RM ANOVA. FDR-adjusted *p*-values are shown for group comparison or interaction. The color-coded scale illustrates the different ranges of mediator release (pg). Abbreviations: ANGPTL4, Angiopoietin-like 4; CCL2/MCP-1, Chemokine C-C motif ligand 2/Monocyte Chemoattractant Protein-1; IDO, Indoleamine 2,3-Dioxygenase; IL-1ra, Interleukin 1 receptor antagonist; IL-4, Interleukin 4; IL-6, Interleukin 6;; IL-8, Interleukin 8; IL-10, Interleukin 10; IL-13, Interleukin 13; IL-18, Interleukin 18; IL-33, Interleukin 33; NA, not available.

showed a lower concentration in the perfusates collected during liver NMP compared to that observed in the liverless perfusion procedures.

The EVs suspended in the perfusates of the liver NMP+bioreactor group ranged from 123.80 nm to 209.2 nm, while a different particle size was revealed in the perfusate samples collected during standard NMP (*p*-value for group comparison: *p* < 0.0001; Supplementary Results 2.4 and Supplementary Fig. 4).

The release of human CK18 was assessed as an index of apoptosis. No significant differences were detected between liverless and liver NMP procedures (*p* = 0.613; Supplementary Results 2.5 and Supplementary Fig. 5).

Liver viability and function during NMP. Hemodynamics monitoring indicated no differences in portal pressures and vascular resistances across experimental groups (*p* = 0.713 and *p* = 0.624, respectively; Supplementary Results 2.6 and Supplementary Fig. 5).

Wash-out samples drained from livers subjected to the bioreactor-based perfusion showed a higher cell count (*p* = 0.008; Fig. 4A) and a greater concentration of nitric oxide (NO)-related metabolites compared to those collected during standard NMP (*p* = 0.016; Fig. 4B).

Analysis of the perfusates withdrawn throughout the procedure revealed a reduced concentration of Alanine-aminotransferase (ALT), Aspartate-aminotransferase (AST), and Lactate dehydrogenase (LDH) in the samples collected during the bioreactor-based perfusion compared to NMP alone (*p*-values for group comparison: AST *p* = 0.016, ALT *p* = 0.008, LDH *p* = 0.0005; Fig. 4c). In line with this observation, the NMP+bioreactor group showed a lower release of the hepatocyte enzyme Arginase-1 (ARG1) and Glutathione Transferase (GST) α relative to standard NMP (Fig. 4d), whereas an opposite trend was observed for the acute-phase response proteins Alpha-1-acid glycoprotein (AGP) and Alpha-2-Macroglobulin (A2M), with greater concentration in samples collected during the bioreactor-based perfusion compared to standard NMP (A2M *p* = 0.043, AGP *p* = 0.033, ARG1 *p* = 0.023, GSTalpha *p* = 0.004; Fig. 4e). In the bioreactor-based perfusion, perfusate pH reached a steady-state starting from 2 h after reperfusion, while a progressive decrease in this parameter was observed in the NMP group (*p* = 0.045; Supplementary Fig. 7). The results obtained from the evaluation of perfusate lactate and electrolytes are provided in Supplementary Results 2.7 and Supplementary Fig. 7.

Livers in the NMP+bioreactor group produced a higher amount of bile compared to standard NMP (0.52 ± 0.04 g bile/g liver vs 0.35 ± 0.03 g bile/g of liver, *p* = 0.013). Bile gas analysis is reported in Supplementary Results 2.8.

Liver edema index was similar across experimental groups (NMP +bioreactor vs NMP: 3.32 ± 0.02 vs 3.18 ± 0.06, *p* = 0.073).

Liver energetics and NAD⁺/NADH ratio. Figure 5a shows the liver tissue Adenosine triphosphate (ATP) content measured at the end of the perfusion procedure. The standard NMP protocol was associated with a lower ATP content compared to both Native (*p* = 0.0001) and SCS groups (*p* = 0.033). Of interest, the bioreactor-based perfusion

a Cells in the wash-out

b Nitrate

c ALT | AST | LDH

d Liver injury

e Liver function
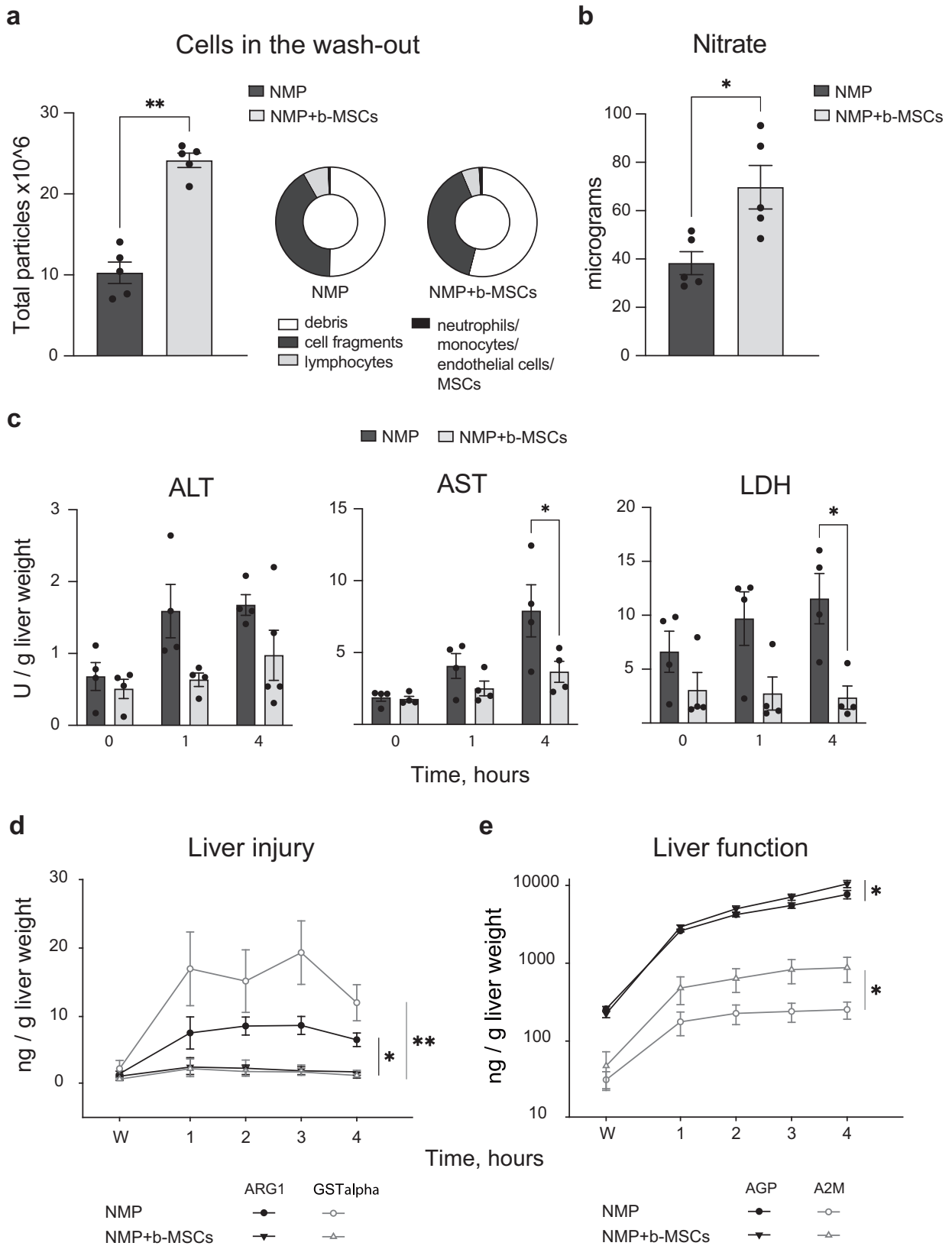
prevented the decrease in ATP associated with reperfusive injury (NMP +bioreactor vs SCS: $p = 0.589$).

Evaluation of ATP breakdown products by high-performance liquid chromatography (HPLC) revealed no difference in energy charge, defined as $(ATP + 0.5 \times ADP) / (ATP + ADP + AMP)$[45], between the NMP and NMP+bioreactor groups (Native: 1.00 ± 0.00, NMP: 0.80 ± 0.03, NMP+bioreactor: 0.82 ± 0.02, $p = 0.347$).

The NMP+bioreactor group showed steady succinate perfusate concentrations throughout the procedure, whereas a dramatic

Fig. 4 | The MSC-bioreactor-based NMP improved rat liver cell viability and function compared to the standard NMP procedure. a The wash-out samples of the NMP+bioreactor group showed a greater donor-derived cell content relative to those collected during standard NMP. Bars denote mean ± SEM, n = 5 biologically independent replicates. Two-sided Mann-Whitney test, *p*-value vs NMP: **p = 0.008. Pie charts show, for each experimental group, the number of particles falling within the following gates: 1) debris, 3-4 μm (NMP+b-MSCs: 54.0% vs NMP: 50.2%); 2) cell fragments, 4.5-6.6 μm (39.7% vs 41.6%) 3) lymphocytes, 7.0-8.0 μm (5.4% vs 7.5%); 4) neutrophils/monocytes/endothelial cells/MSCs, 9-18 μm (1.0% vs 0.7%). **b** In the same wash-out samples, there was an increased concentration of NO metabolites in the bioreactor-based perfusion compared to the NMP group. Bars denote mean ± SEM, n = 5 biologically independent replicates. Two-sided Mann-Whitney test, *p*-value vs NMP: *p = 0.016. **c** Perfusate concentration of clinical hepatocellular damage markers was significantly lower in the NMP+bioreactor group relative to the NMP group. Raw data were adjusted based on circuit volume and liver weight.

Points denote mean ± SEM, n = 4 biologically independent replicates. Two-way RM ANOVA, *p*-value of group comparison: AST *p* = 0.016; ALT *p* = 0.0085; LDH *p* = 0.0005. Tukey's post hoc test was applied for multiple comparisons: asterisks denote *p < 0.05. Immunofluorescence-based analysis indicated that the NMP +bioreactor group showed **d** a reduced release of injury biomarkers and **e** an increased production of acute phase response proteins relative to the NMP group. Raw data were adjusted based on circuit volume and liver weight. Points denote mean ± SEM, n = 5 biologically independent replicates. Two-way RM ANOVA, *p*-value of group comparison: A2M *p* = 0.043; AGP *p* = 0.033; ARG1 *p* = 0.023 (*p* = 0.007 for interaction); GSTalpha *p* = 0.004 (*p* = 0.003 for interaction); Asterisks denote *p < 0.05, **p < 0.01. Abbreviations: A2M, Alpha-2-Macroglobulin; AGP, Alpha-1-acid glycoprotein; ALT, alanine aminotransferase; ARG1, Arginase-1; AST, aspartate aminotransferase; b-MSCs, MSC-bioreactor; GSTalpha, Glutathione Transferase Alpha; LDH, lactate dehydrogenase; NMP, normothermic machine perfusion.
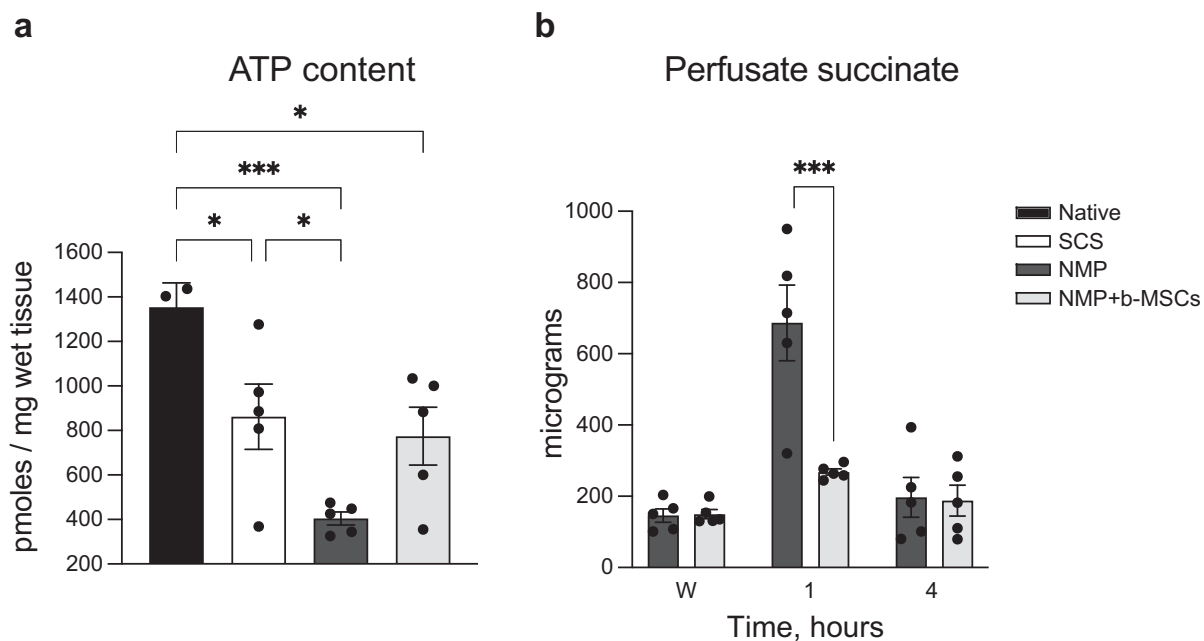
Fig. 5 | The MSC-bioreactor-based perfusion ameliorated rat liver cell mitochondrial function. a While the NMP group showed a decreased ATP content compared to both Native and SCS groups, the bioreactor-based perfusion exhibited a preserved energetic pool, with similar ATP concentration to that observed in the SCS group. Tissue ATP was measured in liver homogenates by bioluminescence-based assay. Raw data were adjusted based on liver weight. Data are expressed as mean ± SEM, n = 5 biologically independent replicates. One-way ANOVA, Tukey's post hoc test. *p*-value: SCS vs Native 0.028; NMP vs Native

p = 0.0001; NMP+b-MSCs vs Native *p* = 0.011; NMP vs SCS *p* = 0.033. Asterisks denote *p < 0.05, ***p < 0.001. **b** The bioreactor-based perfusion reversed the accumulation of succinate induced by cold ischemia. Results were adjusted based on perfusion fluid volume. Data are expressed as mean ± SEM, n = 5 biologically independent replicates. Two-way RM ANOVA, Tukey's post hoc test, *p*-value: ***p = 0.0001. Abbreviations: b-MSCs, MSC-bioreactor; NMP, normothermic machine perfusion; SCS, static cold storage; W, wash-out.

increase in this metabolite was observed in the standard NMP group at 1 h of perfusion (*p* < 0.0001; Fig. 5B).

Tissue Nicotinamide adenine dinucleotide/Nicotinamide adenine dinucleotide+hydrogen (NAD$^+$/NADH) ratio was similar across experimental groups (NMP+bioreactor: 1.52 ± 0.15 vs NMP: 1.49 ± 0.11, *p* = 0.783). However, the bioreactor-based perfusion was associated with increased content of both NAD$^+$ (*p* < 0.001) and NADH (*p* = 0 = 0.0007) compared to the NMP alone (Supplementary Results 2.9 and Supplementary Fig. 8).

Immunonomodulatory effects exerted by the MSC-derived secretome. The bioreactor-based perfusion was associated with a broad modulation of mediators relevant to inflammation and its resolution (Fig. 6). Intercellular Adhesion Molecule 1 (ICAM-1, *p* = 0.039), Vascular Endothelial Growth Factor (VEGF, *p* < 0.001), and the

chemokines Chemokine C-C motif ligand 5/regulated on activation normal T cell expressed and secreted (CCL5/RANTES, *p* = 0.018), C-X-C motif chemokine ligand 1/Growth-regulated protein α (CXCL1/GROα, *p* = 0.047), C-X-C Motif Chemokine Ligand 10/Interferon gamma-induced protein 10 (CXCL10/IP-10, *p* = 0.010) were downregulated in perfusates from the NMP+bioreactor group compared to standard NMP. Conversely, samples collected from livers exposed to MSC-derived secretome exhibited a greater concentration of IL-6 (*p* = 0.015), Tumor necrosis factor (TNF)-α (*p* = 0.035), Chemokine C-C motif ligand 3/Macrophage Inflammatory Protein-1α (CCL3/MIP-1α, *p* = 0.022), and C-X-C Motif Chemokine Ligand 5/Lipopolysaccharide-induced CXC chemokine (CXCL5/LIX, *p* = 0.013). Moreover, there was a marked induction of Adiponectin (*p* < 0.001), Hepatocyte growth factor (HGF, *p* = 0.014), and Connective Tissue Growth Factor (CTGF, *p* < 0.001).

NMP+b-MSCs vs NMP

Pattern	Mediator	1h	2h	3h	4h	p-value
Inflammation and leukocyte recruitment						
	CCL5/RANTES	-1.3	-1.1	-1.1	-0.7	**0.018**
	CXCL1/GROa	-0.6	-0.6	-0.8	-1.3	**0.047**
	CXCL10/IP-10	-0.8	-1.4	-0.8	-0.9	**0.010**
	IL-18	-0.4	-0.4	-0.1	-0.5	0.146
	sICAM-1	-0.2	-0.6	-1.5	-0.5	**0.039**
	VEGF	0.1	-0.1	-0.4	-0.5	**<0.001#**
	CCL2/MCP-1	0.4	0.1	0.2	0.2	0.172
	CCL3/MIP-1a	0.6	1.1	0.9	1.1	**0.022**
	CXCL5/LIX	0.5	0.6	0.1	0.1	**0.013#**
	IL-6	0.5	0.6	0.6	0.6	**0.015**
	INF-gamma	0.4	0.5	0.6	0.5	0.089
	TNF-alpha	-0.1	0.2	0.9	1.1	**0.035#**
Inflammation resolution and liver cell regeneration						
	Adiponectin	2.7	2.6	2.5	2.1	**<0.001**
	CTGF	0.8	0.8	0.8	0.8	**<0.001**
	HGF	1.5	1.3	1.4	1.4	**0.014**
	IL-4	0.2	0.6	0.6	0.5	0.175
	IL-10	-0.4	-0.1	0.2	0.2	0.342
	IL-13	2.2	0.7	0.6	0.0	0.285
	TIMP-1	0.9	0.6	0.6	0.8	**<0.001**
	FC scale	-3.0	-1.5	0.0	1.5	3.0

Fig. 6 | Immunomodulating and pro-resolving effects associated with the MSC-bioreactor perfusion. Perfusate profiling indicated that the bioreactor-based NMP induced a broad modulation of several factors involved in inflammation and leukocyte recruitment, inflammation resolution, and liver cell regeneration. Raw data were adjusted based on circuit volume and liver weight. Results are expressed as log2-transformed fold change between the NMP+bioreactor group and the NMP group at each time point. Five independent replicates were analyzed for each experimental condition. Two-way RM ANOVA, followed by Tukey's post hoc test. The color-coded scale illustrates the diverse magnitudes of fold change. Abbreviations: b-MSCs, MSC-bioreactor; CCL2/MCP-1, Chemokine C-C motif ligand 2/Monocyte Chemoattractant Protein-1; CCL3/MIP-1α, Chemokine C-C motif ligand 3/Macrophage Inflammatory Protein-1α; CCL5/RANTES, Chemokine C-C motif ligand 5/regulated on activation normal T cell expressed and secreted; CTGF, Connective Tissue Growth Factor; CXCL-1/GRO α, C-X-C Motif Chemokine Ligand 1/Growth-regulated protein α; CXCL5/LIX, C-X-C Motif Chemokine Ligand 5/Lipopolysaccharide-induced CXC chemokine; CXCL10/IP-10, C-X-C Motif Chemokine Ligand 10/Interferon gamma-induced protein 10; FC, Fold change; HGF, Hepatocyte growth factor; IFN-γ, Interferon-γ; IL-4, Interleukin 4; IL-6, Interleukin 6; IL-10, Interleukin 10; IL-13, Interleukin 13; IL-18, Interleukin 18; NMP, normothermic machine perfusion; TIMP-1, Tissue Inhibitor of Metalloproteinase 1; TNF-α, Tumor Necrosis Factor-α; sICAM-1, soluble Intercellular Adhesion Molecule-1; VEGF, Vascular Endothelial Growth Factor.

Characterization of the MSCs harvested from the bioreactor after liver NMP. MSCs flow cytometry analysis is presented in Supplementary Results 2.10.

Bioreactor-based liver NMP in a large animal model
To upscale the cell number according to circuit volume and porcine liver weight, the bioreactor was prepared using a human plasmafilter (Aferetica srl, Supplementary Fig. 9) and a total of 3.7×10^7 MSCs was used. Cell isolation and culturing were performed following the same procedure adopted for the small animal model (Supplementray methods 1.1).

The bioreactor was integrated to the arterial side of the Liver Assist® (XVIVO Perfusion AB) perfusion platform. More specifically, a dedicated loop was connected to the standard circuit downstream a membrane lung oxygenator (Supplementary Fig. 10).

Livers were subjected to 1 h warm ischemia in situ, followed by 30 min cold ischemia (Supplementary methods 1.11). Mean liver weight was 1312 ± 78 g.

During the NMP procedure, all livers were hemodynamically stable, with no difference in portal vein (PV) and hepatic artery (HA) flows and vascular resistances between experimental groups (Fig. 7a and b. HA flow and resistance: $p = 0.151$ and $p = 0.285$; PV flow and resistance: $p = 0.901$ and $p = 0.334$). No clotting formation was observed.

Perfusate lactate concentration significantly decreased over time in both the NMP+bioreactor and NMP groups (Fig. 7c, p-value for time $p < 0.00001$, p-value for group $p = 0.563$). No differences were observed in perfusate pH (Supplementary Fig. 11, $p = 0.233$).

Hepatonecrosis biomarker (Fig. 7d, Supplementary Table 4), electrolyte composition (Supplementary Table 5), and biochemical parameters (Supplementary Table 4) were similar across experimental groups at any time points. Bile production started at 1 h with a mean output of 12 ml/h ($p = 0.636$).

Histological examination of tissue biopsies collected at the end of the perfusion procedure showed no signs of parenchymal damage (Supplementary Fig. 12) or liver injury (Supplementary Table 6).

Cells enzymatically detached from the bioreactors at the end of perfusion were viable and able to proliferate in vitro. Flow cytometry indicated a preserved expression of stemness markers, while a neglibile surface expression of endothelial markers was observed ($0.10 \pm 0.03\%$ CD45-/34+/31-; $0.07 \pm 0.02\%$ CD45-/34+/31+; $0.39 \pm 0.13\%$ CD45-/34-/31+; $97.35 \pm 0.92\%$ CD45-/34-/31-/90+; $95.95 \pm 1.21\%$ CD73+; $94.8 \pm 1.52\%$ CD105+; $98.29 \pm 0.47\%$ CD29+).

Discussion

The present research implemented an innovative platform for the application of MSC-based therapies during NMP. An in vitro study was initially performed to test the functionality and stability of the novel NMP system integrated with a hollow fiber bioreactor seeded with adipose tissue-derived MSCs. Next, the small animal study demonstrated that, compared to standard NMP, the MSC-bioreactor-based perfusion mediated a more efficient hepatic reperfusion, enhanced liver viability, improved hepatic cell energetic status, and induced the release of pro-resolving and pro-regenerative factors. Finally, the pilot study conducted using porcine livers proved that MSC-bioreactors can be safely incorporated into NMP platforms commonly used in clinical practice and that the novel configuration can support the protocol for human liver NMP.

The main focus was to establish and optimize an unprecedented technology where the NMP perfusion system is coupled with a MSC-bioreactor. To achieve this, the research followed a stepwise approach: starting from in vitro experiments for developing the novel setup, then progressing to a small animal study to explore the interaction between MSCs and the liver, and finally culminating in a pilot feasibility study using porcine livers and a clinical NMP platform. The ultimate aim was to improve the application of cell-based therapies during NMP, while avoiding any drawback related to stem cell direct administration into the perfusion fluid[17,30,31]. In this regard, the in vitro study demonstrates that MSCs can be cultured in hollow fiber bioreactors, shipped to other facilities, and then be subjected to a perfusion procedure without affecting their core stem properties. This workflow offers the cells the opportunity to recover from freezing/thawing, a process that significantly impairs MSCs survival and their cytoprotective activity[30]. Moreover, in addition to ensuring optimal stem cell culturing conditions during NMP, the use of a bioreactor completely prevents MSCs adherence to the circuit, which reduces therapeutic effectiveness[46].

A key finding of the present research is that the liver-related inflammatory factors, released during NMP, boosted the activation of the MSCs' secretory activity. In fact, the specific configuration of our platform allowed a bidirectional communication between the liver and MSCs, enabling the stem cells to be primed with the perfusate enriched by the signaling and damage molecules secreted from hepatic cells. This liver-driven licensing of MSCs led to the release of a tailored secretome. As an example, the higher release of IL-10, IL-1ra, and IL-4
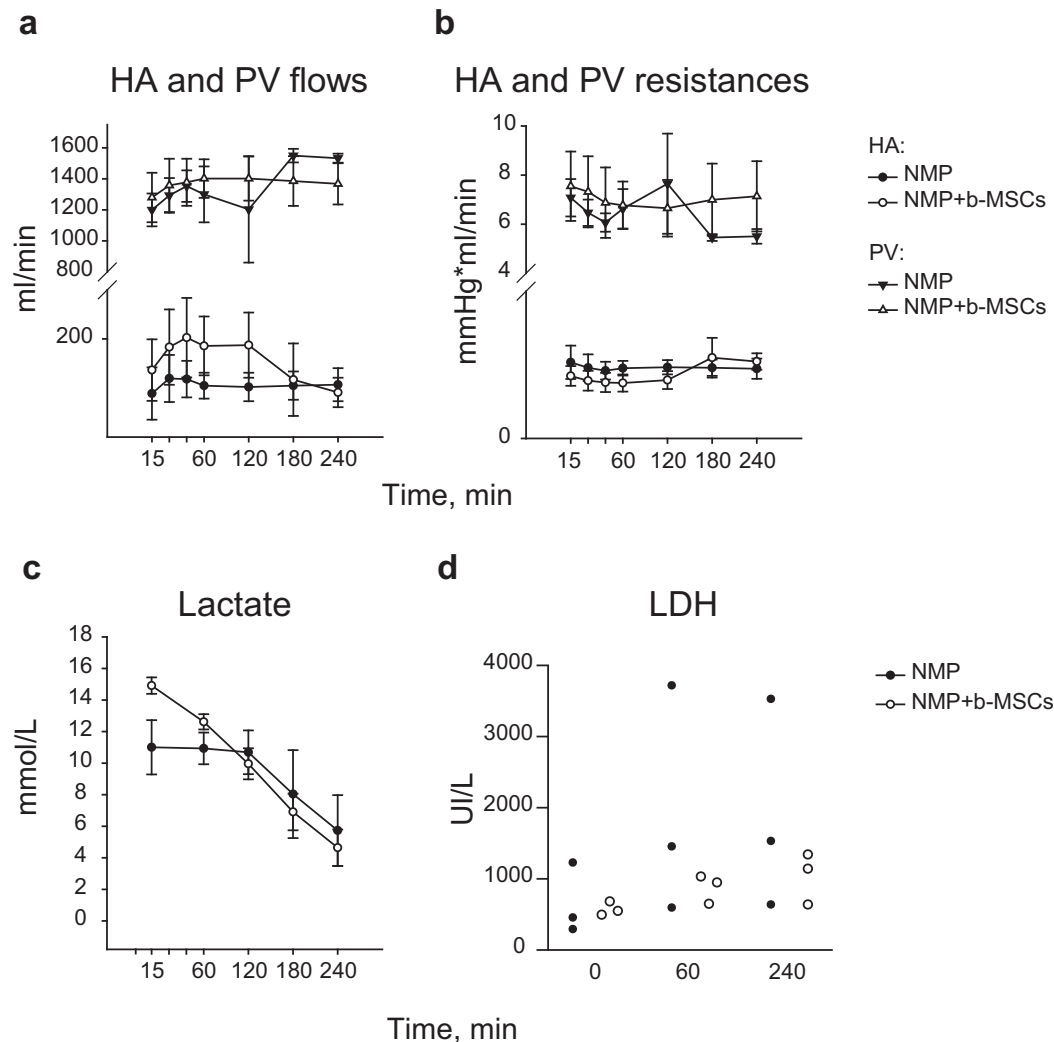
Fig. 7 | MSC-bioreactor-based liver NMP in a large animal model. In this pilot study, livers procured from donor swines were subjected to 4 h-NMP using the Liver Assist® (XVIVO Perfusion AB) device equipped with MSC-bioreactors (n = 3). The results were compared to those obtained from standard porcine liver NMP (n = 3). The collected data clearly indicate that the MSC-bioreactor can be safely integrated into a perfusion device currently available for the clinical setting. No difference in vascular **a** flows and **b** resistances was observed between livers subjected to the bioreactor-based perfusion compared to those exposed to the standard NMP. Points denote mean ± SEM, n = 3 biologically independent replicates. Two-way RM ANOVA; p-value between experimental groups: HA flow $p = 0.151$; HA resistance $p = 0.285$; PV flow $p = 0.901$; PV resistance $p = 0.334$. **c** Lactate clearance was similar across experimental groups. Points denote mean ± SEM, n = 3 biologically independent replicates. Two-way RM ANOVA; $p = 0.563$. **d** Perfusate LDH concentration tended to be lower in the NMP+bioreactor group. Points denote each experimental unit, n = 3 biologically independent replicates. Two-way ANOVA, $p = 0.064$. Abbreviations: b-MSCs, MSC-bioreactor; HA, hepatic artery; LDH, lactate dehydrogenase; NMP, normothermic machine perfusion; PV, portal vein.

observed in the context of liver NMP, compared to the liverless procedure, suggests that MSCs responded to the liver factors by promoting an anti-inflammatory and pro-resolving environment.

Compared with standard NMP, the bioreactor-based perfusion exerted multiple beneficial effects which enabled to counteract many of the harmful events triggered by organ donation, cold storage, and reperfusion at normothermia. In fact, a reduced release of injury biomarkers, a greater bile output, and an increased concentration of acute-phase proteins were observed. In addition, during the initial reperfusion phase, the wash-out of donor blood was more effective in livers exposed to the MSC-derived secretome, likely as a consequence of the increased availability of the vasodilator NO[47]. Although a direct comparison with human liver reference viability criteria[12,48] cannot be performed due to the obvious differences between clinical and preclinical protocols, our results demonstrate that exposure the bioreactor-based perfusion limited cell death and improved the recovery of liver biosynthetic activity.

Another significant effect involves liver cell energetics and mitochondrial function. Indeed, MSC treatment protected from the ATP depletion typically induced by IR[49]. This observation is of paramount importance for the transplantation setting, as ATP pool exhaustion is a crucial event leading to ion homeostasis failure, cell swelling, and, ultimately, apoptosis activation within ischemic cells[49–51]. The absence of succinate accumulation in livers exposed to the MSC-derived secretome further supports the positive impact of the bioreactor-based perfusion on tissue energetics. A dysregulated increase in this metabolite has been previously documented in liver grafts subjected to an ischemic challenge[42,52] and represents a key indicator of disrupted cellular energy metabolism[53]. Consistently, a rapid metabolization of the accumulated succinate, as seen during hypothermic oxygenated perfusion (HOPE)[52], arose as an effective intervention strategy against IRI[54,55]. The concomitant ATP recovery and succinate removal observed in this study, suggest a broader positive influence exerted by MSCs on the mitochondrial electron transfer chain. Stem cell ability to transfer viable

mitochondria to injured cells[56,57] could have a role in the restoration of injured cell energetic status. Further studies are required to determine whether this intriguing mechanism contributes to the protection conferred by MSCs in the context of hepatic IRI.

Liver exposure to the MSC-derived secretome was associated with substantial changes in the perfusate inflammatory profile. Compared to standard NMP, the NMP+bioreactor group exhibited a reduced release of different inflammatory mediators, whereas higher concentrations of IL-6, TNF-α, and certain chemokines were observed. This molecular scenario depicts a coordinated adaptive response to the reperfusive injury. In fact, TNF-α and IL-6 are secreted as part of the pathophysiological immune response to ischemia[58,59], to induce leukocyte recruitment to the injured site, tissue repair, and damaged cell removal[50]. In addition, TNF-α and IL-6 are key factors in liver cell regeneration[60]. Consistently, higher serum concentrations of these molecules were associated with improved graft regeneration after liver transplantation[61]. In addition, in livers subjected to the bioreactor-based perfusion there was a higher release of various protective factors, including Adiponectin, CTGF, HGF, and, during the initial stage after reperfusion, IL-13. The induction of Adiponectin appears particularly interesting, due to its well-known properties in the mitigation of inflammation and oxidative stress in the context of liver diseases[62–64]. Similarly, the increase in HGF could significantly contribute to IRI resolution, as this potent mitogen promotes the regeneration of hepatocytes as well as of biliary and liver endothelial cells[65]. Overall, these findings indicate that MSC-based therapy exerted a broad impact on different aspects of immune homeostasis, including the recruitment of leukocytes to control inflammation[21], and, at the same time, it mediated the induction of endogenous protective pathways to counteract the deleterious events triggered by IR.

The information acquired in the small animal model was successfully translated to guide the integration of this innovative setup into a commercially-available perfusion device approved for clinical perfusion. The data collected in our pilot study involving porcine livers clearly indicate the feasibility and safety of integrating MSC-bioreactors into the NMP protocols for human use. These preliminary findings support the technical feasibility of coupling a MSC-bioreactor into a clinical NMP circuit and provide a solid foundation for future studies aimed at investigating the clinical translability of our advanced perfusion platform. Of note, the availability of new strategies for stem cell upscaling and manufacturing[66] could facilitate the translational use of our novel technology in a human setting.

The study shows some limitations that warrant further discussion. 1) In vitro study (WP1): we acknowledge minor weaknesses in the bioreactor preparation workflow. In fact, MSCs experienced a certain degree of oxidative stress during shipment. This observation underscores the possible need to supplement the culture medium with antioxidants (e.g. vitamin C, glutathione). Moreover, due to a low efficiency in MSC detachment from the bioreactor fibers, we could not provide the exact number of the cells present in the device after NMP. 2) Small animal study (WP2): we used livers exposed to a short cold ischemia time to reduce potential confounding factors and, as a consequence, to gain a clearer understanding of the biological processes elicited by the bioreactor-based perfusion. The adopted experimental setting did successfully reproduce the key pathophysiological features of liver IR injury and enabled to observe the benefits conferred to the liver. We believe that the investigation of the long-term effects of the bioreactor-based perfusion in transplanted livers represents a logical next step of the present research, that could be used as useful starting point for future targeted studies. In fact, the strict application of the PREPARE and the "Animal Research: Reporting of In Vivo Experiments" (ARRIVE) guidelines[43,67] ensures the reproducibility of our investigation, thereby facilitating research advancement by other

Research groups. 3) Large animal study (WP3): this pilot study follows a feasibility design and, as such, has a limited sample size. Moreover, it was not intended to provide conclusive results on the translability of the bioreactor-based perfusion, but only to demonstrate that the new circuit configuration could safely support the protocol for human liver MP. Of note, the progression towards a setting similar to the human scenario required significant protocol adjustments and circuit modifications compared to the small animal study. These changes prevented the possibility of performing a direct comparison of the MSCs' effects on rat and pig livers, which, however, was already outside the scope of our pilot study. 4) WP2 and WP3: The selected perfusion time was optimal to explore the MSC-bioreactor effects on initial IRI[42,52,68] and enabled to successfully demonstrate the technical feasibility of integrating the device into the NMP circuit. We acknowledge that a deeper investigation of the pathophysiological consequences of the bioreactor-based perfusion would have required a more prolonged perfusion. However, extended perfusion time is associated with unavoidable changes in liver cell metabolism, as recently reported by our group[44], and, therefore requires further implementation before being implemented for organ treatment.

In conclusion, the present proof-of-concept study demonstrates, for the first time, that the integration of a MSC-bioreactor into a NMP platform is feasible and effective in reducing the initial IRI. Thanks to a stepwise experimental workflow, ranging from in vitro evaluations to preclinical models, the research presents several innovative findings that, in our view, could support further relevant advancements in the field. In fact, the use of a bioreactor to avoid a direct contact between MSCs and the organ represents a significant breakthrough, as it addresses the common drawbacks related to MSC applications[32–34]. Besides implementing an unprecedented perfusion circuit, our small animal study proves, for the first time, that the well-documented beneficial effects of stem cells can be achieved even in this particular setting. Another noteworthy achievement of our investigation is represented by the induction of a liver-tailored reprogramming of stem cells' secretory activity, that could overcome the negative impact of inadequate cell licensing on MSC efficacy[38]. Finally, the pilot study in porcine livers provides feasibility evidence indicating that the novel technology can be upscaled to a large animal set-up resembling the clinical situation. The data provided by the present research represent pivotal information for a future development of cutting-edge platforms for ex situ organ repair. A deeper understanding of the therapeutic potential of the bioreactor-based perfusion will require targeted investigation in both preclinical models of graft injury and non-viable human livers. This perspective becomes even more intriguing when considering the latest advancements in prolonged perfusion protocols documented by our group[44,69,70] and others[71–74]. Another promising approach to further explore the impact of the bioreactor-based perfusion could involve the use of split livers, which could provide valuable information on the effects exerted by stem cells on injured versus non-injured liver parenchyma.

Methods

Development of the advanced NMP platform for rat liver NMP coupled with the MSC-bioreactor

MSC-bioreactor preparation and preliminary analysis. MSCs were obtained from human adipose tissue under approval number 2892 P, released by Padua Ethical Committee for Clinical Research on 10/06/2013. Methods for cell isolation and culturing in vitro are described in Supplementary methods 1.1. A preliminary characterization of the MSCs is provided in Supplementary results 2.1.

The hollow fiber bioreactors (Aferetica srl, Supplementary Information 1.2 and Supplementary Fig. 1) show a cylindrical

structure containing bundles of polysulfone fibers that create a surface area suitable for cell growth. There are two distinct compartments: the intracapillary space, which is inside the hollow fibers, and the extracapillary space, which surrounds the fibers within the chamber. The fibers provide a total culturing surface of 500 cm^2 and are composed of membranes with pores measuring 150 nm in diameter.

A total of 2×10^7 MSCs were injected into the extracapillary space of the bioreactor at a seeding density of 4×10^4 cells/cm^2. After 12 h-incubation at standard conditions, supernatants were replaced with complete medium and MSC-bioreactors were shipped at room temperature to Milan.

Once received at the Milan lab, supernatants were replaced with fresh medium. Collected supernatants were analyzed by gas analysis (ABL 800 Flex, Radiometer Medical ApS, Copenhagen, Denmark) and then stored at -80 °C for bio-molecular analysis. Cell pellets were counted with an automated cell counter (Scepter™, Millipore Corporation, Merck KGaA, Darmstadt, Germany) and analyzed using the Scepter™ 2.0 software pro (Merck KGaA).

Liverless-NMP. The MSC-bioreactors were kept at standard culturing conditions for 24-48 h. Then, the bioreactors were connected to a customized circuit derived from an isolated lung perfusion system (Hugo Sachs Elektronik, Harvard Apparatus, March-Hugstetten, Germany)[75].

A description of the protocol and the materials used is provided in the Supplementary methods 1.3. The system was primed with perfusion fluid supplied with an oxygen carrier (Oxyglobin®, HBO2 Therapeutics, Boston, USA). After connecting the bioreactors to the circuit, the perfusion fluid was pumped inside the bioreactor with a flow rate of 20 ml/min. The perfusion was maintained for 4 h and involved continuous pressure and temperature monitoring with hourly evaluation of perfusate acid-base balance, electrolytes, and metabolite concentration.

Perfusate samples collected throughout NMP were adequately processed to evaluate the concentration of the parameters listed in Supplementary methods 1.3, and in 1.9. The amount and size of EVs in the perfusates were assessed as described in the Supplementary methods 1.9.

At the end of liverless-NMP, MSCs were enzymatically harvested, counted, and analyzed by flow-cytometry (Supplementary methods 1.4).

Bioreactor-based liver NMP in a rat model
Experimental groups. Twenty rats were randomly assigned to one of the following experimental groups (n = 5 each, Supplementary Table 1): 1) Native, livers were procured from rats in resting conditions; 2) SCS, livers were flushed in-situ, procured, and subjected to 30 min-cold storage; 3) NMP, livers were treated as the SCS group and then ex situ perfused for 4 h using the standard perfusion platform; 4) NMP+bioreactor, livers were treated as the SCS group and then ex situ perfused for 4 h using the MSC-bioreactor-equipped platform.

Rat model. The procedures involving the use of laboratory animals were performed at the Center for Preclinical Research, under the authorization number 456/2021 (issuing date: June 22nd, 2021). Sprague–Dawley male rats (Charles River, Calco, Lecco, Italy) weighing 250-300 g were housed in a ventilated cage system (Tecniplast, S.p.A., Varese, Italy) at 22 ± 2°C, 55 ± 10% humidity, on a 12 h dark/light cycle, and were allowed free access to feed and water.

Methods for anesthesia induction, surgery, in-situ flushing with an ice-cold preservation solution, and liver procurement are described in the Supplementary methods 1.6.

Normothermic liver machine perfusion. Liver perfusion was performed as reported in the Supplementary methods 1.7. Hemodynamics parameters were monitored throughout the procedure (ADInstruments, Dunedin, New Zeland). Perfusate and bile gas analysis was hourly performed (ABL 800 Flex).

Sample collection and bio-molecular analysis. A description of sample collection is provided in the Supplementary Table 3. Briefly, during the first 5 min of NMP, the entire volume (20 ml) of the outflow perfusate was withdrawn from the vena cava "wash-out". Then, samples of the recirculating perfusate were collected hourly and processed as previously described[76,77] and as reported in Supplementary methods 1.8. A list of the parameters evaluated is provided in Supplementary methods 1.9 and 1.10.

Bile was collected into a test tube containing 200 μL of vaseline and weighted to estimate bile production and analyzed with a gas analyzer.

Liver biopsies were obtained from the right median lobe at the end of NMP. One sample was used to assess wet-to-dry ratio (edema index), one was formalin-fixed, while the others were snap-frozen and stored at -80 °C for subsequent evaluation of ATP content and NAD$^+$/NADH ratio (Supplementary methods 1.11).

Bioreactor-based liver NMP in a large animal model
Porcine model and experimental groups. The procedures involving the use of swines were performed at the Department of Veterinary Medical Sciences (Ozzano, Italy), under the authorization number 2216 A.N.AB.

Swines weighting 62-87 Kg were randomly assigned to one of the following experimental groups: 1) NMP (n = 3), livers exposed to 1 h-warm ischemia, flushed in-situ, procured, and subjected to 30 min-cold ischemia and then ex situ perfused for 4 h using the standard Liver Assist® perfusion platform (XVIVO Perfusion AB); 2) NMP+bioreactor (n = 3), livers were treated as the NMP group and then ex situ perfused for 4 h using the Liver Assist® perfusion platform equipped with a MSC-bioreactor.

Preparation of the bioreactor suitable for porcine livers. Bioreactors were prepared following the same procedure developed for the small animal model (Supplementary methods 1.1 and 1.12). Briefly, after cell expansion in vitro, a cell suspension at a concentration of 1.85×10^6 cells/ml were injected into human plasmafilters (Aferetica srl, Supplementary Fig. 10). The bioreactors share similar characteristics with the device used in the small animal study, except for a greater total volume capacity The final seeding density in the device was 1.85×10^4 cells/cm^2.

Normothermic liver machine perfusion. A description of the porcine donation model and the protocol used for porcine NMP is provided in the Supplementary methods 1.12.

Statistical analysis
Sample size for the rat model was calculated by a priori power analysis, in compliance with the 3 R principles[78,79] and the PREPARE guidelines[43]. Details are provided in the Supplementary methods 1.5, following the scheme established by the ARRIVE guidelines[67]. The pilot study in large animals was conducted to test the feasibility of bioreactor integration into a commercially-available circuit for human use. Sample size was determined according to the guidance published by NC3R[80] (Supplementary methods 1.12).

Data are presented as mean ± standard error of the means (SEM) or median [25–75th percentile]. Differences across experimental groups were investigated using the one-way analysis of variance (ANOVA) or two-way repetitive measures (RM) ANOVA, followed by Tukey's post hoc test for multi-comparison procedures. p-values were adjusted using the Benjamini-Hochberg (BH) procedure to control the False Discovery Rate (FDR). Non-normally distributed data were rank-

transformed before ANOVA. A probability value of $p < 0.05$ was considered significant. The tests were performed using SigmaStat software 11.0 (Systat Software Inc, San Jose, CA, USA), Prism 9 (GraphPad Software, LCC, CA, USA), and JMP Pro 17.2.0 (JMP Statistical Discovery LLC, SAS Campus Drive, NC, USA).

Reporting summary

Further information on research design is available in the Nature Portfolio Reporting Summary linked to this article.

Data availability

All data generated or analysed during this study are included either in the present article, its supplementary information files, or at 10.5281/zenodo.14013781. Any additional requests for information can be directed to, and will be fulfilled by the corresponding authors.

References

1. Parente, A. et al. Machine perfusion techniques for liver transplantation - A meta-analysis of the first seven randomized controlled trials. *J. Hepatol*. https://doi.org/10.1016/J.JHEP.2023.05.027 (2023).
2. Liew, B. et al. Liver transplant outcomes after ex vivo machine perfusion: a meta-analysis. *Br. J. Surg*. **108**, 1409–1416 (2021).
3. Lonati, C. et al. Influence of *ex vivo* perfusion on the biomolecular profile of rat lungs. *FASEB J*. fj.201701255R (2018).
4. Jassem, W. et al. Normothermic machine perfusion (nmp) inhibits proinflammatory responses in the liver and promotes regeneration. *Hepatology* **70**, 682–695 (2019).
5. Gatti, S. et al. Reduced expression of the melanocortin-1 receptor in human liver during brain death. *Neuroimmunomodulation* **13**, 51–55 (2006).
6. Ghinolfi, D. et al. Sequential use of normothermic regional and ex situ machine perfusion in donation after circulatory death liver transplant. *Liver Transplant*. **27**, 385–402 (2021).
7. Catania, A., Lonati, C., Sordi, A. & Gatti, S. Detrimental consequences of brain injury on peripheral cells. *Brain. Behav. Immun*. **23**, (2009).
8. Czigany, Z.et al. Hypothermic Oxygenated Machine Perfusion (HOPE) Reduces Early Allograft Injury and Improves Post-Transplant Outcomes in Extended Criteria Donation (ECD) Liver Transplantation from Donation After Brain Death (DBD). *Ann. Surg*. **Publish Ah**, (2021).
9. Patrono, D. et al. Clinical assessment of liver metabolism during hypothermic oxygenated machine perfusion using microdialysis. *Artif. Organs* 1–15 https://doi.org/10.1111/aor.14066 (2021).
10. Schlegel, A., Kron, P., Graf, R., Dutkowski, P. & Clavien, P. A. Warm vs. cold perfusion techniques to rescue rodent liver grafts. *J. Hepatol*. **61**, 1267–1275 (2014).
11. Gaurav, R. et al. Liver Transplantation Outcomes from Controlled Circulatory Death Donors: SCS vs in situ NRP vs ex situ NMP. *Ann. Surg*. **275**, 1156–1164 (2022).
12. Mergental, H. et al. Transplantation of discarded livers following viability testing with normothermic machine perfusion. *Nat. Commun*. **11**, (2020).
13. Nasralla, D. et al. A randomized trial of normothermic preservation in liver transplantation. (2018).
14. Lonati, C. et al. Effluent Molecular Analysis Guides Liver Graft Allocation to Clinical Hypothermic Oxygenated Machine Perfusion. 1–18 (2021).
15. Panconesi, R. et al. Impact of Machine Perfusion on the Immune Response After Liver Transplantation - A Primary Treatment or Just a Delivery Tool. *Front. Immunol*. **13**, (2022).
16. Roushansarai, N. S., Pascher, A. & Becker, F. Innate Immune Cells during Machine Perfusion of Liver Grafts — The Janus Face of Hepatic Macrophages. (2022).
17. Li, J. et al. Application of Mesenchymal Stem Cells During Machine Perfusion: An Emerging Novel Strategy for Organ Preservation. *Front. Immunol*. **12**, 1–16 (2021).
18. Bogensperger, C. et al. Ex vivo mesenchymal stem cell therapy to regenerate machine perfused organs. *Int. J. Mol. Sci*. **22**, (2021).
19. Podestà, M. A., Remuzzi, G. & Casiraghi, F. Mesenchymal Stromal Cell Therapy in Solid Organ Transplantation. *Front. Immunol*. **11**, 1–12 (2021).
20. Hoogduijn, M. J. et al. The emergence of regenerative medicine in organ transplantation: 1st European Cell Therapy and Organ Regeneration Section meeting. *Transpl. Int*. **33**, 833–840 (2020).
21. Mansourabadi, A. H., Mohamed Khosroshahi, L., Noorbakhsh, F. & Amirzargar, A. Cell therapy in transplantation: A comprehensive review of the current applications of cell therapy in transplant patients with the focus on Tregs, CAR Tregs, and Mesenchymal stem cells. *Int. Immunopharmacol*. **97**, 107669 (2021).
22. Saidi, R. F. et al. Human adipose-derived mesenchymal stem cells attenuate liver ischemia-reperfusion injury and promote liver regeneration. *Surg. (U. S.)* **156**, 1225–1231 (2014).
23. Chen, K. et al. Adipose-derived mesenchymal stromal / stem cell line prevents hepatic ischemia / reperfusion injury in rats by inhibiting inflammasome activation. https://doi.org/10.1177/09636897221089629 (2022).
24. Sasajima, H. et al. Cytoprotective effects of mesenchymal stem cells during liver transplantation from donors after cardiac death in rats. *Transplant. Proc*. **50**, 2815–2820 (2018).
25. Yang, L. et al. Normothermic machine perfusion combined with bone marrow mesenchymal stem cells improves the oxidative stress response and mitochondrial function in rat donation after circulatory death livers. *Stem Cells Dev*. **29**, 835–852 (2020).
26. Yang, L. et al. Bone marrow mesenchymal stem cells combine with normothermic machine perfusion to improve rat donor liver quality—the important role of hepatic microcirculation in donation after circulatory death. *Cell Tissue Res*. **381**, 239–254 (2020).
27. Sun, D. et al. Protective effects of bone marrow mesenchymal stem cells (BMMSCS) combined with normothermic machine perfusion on liver grafts donated after circulatory death via reducing the ferroptosis of hepatocytes. *Med. Sci. Monit*. **27**, 1–13 (2021).
28. De Stefano, N. et al. Human liver stem cell-derived extracellular vesicles reduce injury in a model of normothermic machine perfusion of rat livers previously exposed to a prolonged warm ischemia. *Transpl. Int*. **34**, 1607–1617 (2021).
29. Tian, X. et al. Heme oxygenase-1-modified bone marrow mesenchymal stem cells combined with normothermic machine perfusion repairs bile duct injury in a rat model of dcd liver transplantation via activation of peribiliary glands through the wnt pathway. *Stem Cells Int*. **2021**, (2021).
30. Sierra Parraga, J. M. et al. Effects of normothermic machine perfusion conditions on mesenchymal stromal cells. *Front. Immunol*. **10**, 1–11 (2019).
31. Deng, B. et al. Removal from adherent culture contributes to apoptosis in human bone marrow mesenchymal stem cells. *Mol. Med. Rep*. **15**, 3499–3506 (2017).
32. Gleeson, B. M. et al. Bone marrow-derived mesenchymal stem cells have innate procoagulant activity and cause microvascular obstruction following intracoronary delivery: amelioration by antithrombin therapy. *Stem Cells* **33**, 2726–2737 (2015).

33. Brasile, L. & Stubenitsky, B. Will cell therapies provide the solution for the shortage of transplantable organs? *Curr. Opin. Organ Transplant.* **24**, 568–573 (2019).

34. Haarer, J., Johnson, C. L., Soeder, Y. & Dahlke, M. H. Caveats of mesenchymal stem cell therapy in solid organ transplantation. *Transpl. Int.* **28**, 1–9 (2015).

35. Grange, C., Bellucci, L., Bussolati, B. & Ranghino, A. Potential applications of extracellular vesicles in solid organ transplantation. *Cells* **9**, 1–13 (2020).

36. Burja, B. et al. Human mesenchymal stromal cells from different tissues exhibit unique responses to different inflammatory stimuli. *Curr. Res. Transl. Med.* **68**, 217–224 (2020).

37. Marigo, I. & Dazzi, F. The immunomodulatory properties of mesenchymal stem cells. *Semin. Immunopathol.* **33**, 593–602 (2011).

38. Krampera, M. Mesenchymal stromal cell licensing: A multistep process. *Leukemia* **25**, 1408–1414 (2011).

39. Alagesan, S. et al. Enhancement strategies for mesenchymal stem cells and related therapies. *Stem Cell Res. Ther.* **13**, 1–16 (2022).

40. Lonati, C. et al. Mesenchymal stem cell–derived extracellular vesicles improve the molecular phenotype of isolated rat lungs during ischemia/reperfusion injury. *J. Hear. Lung Transplant.* https://doi.org/10.1016/j.healun.2019.08.016 (2019).

41. Dondossola, D. et al. Human Red Blood Cells as Oxygen Carriers to Improve Ex-Situ Liver Perfusion in a Rat Model. *J. Clin. Med.* https://doi.org/10.3390/jcm8111918 (2019).

42. Lonati, C. et al. Quantitative Metabolomics of Tissue, Perfusate, and Bile from Rat Livers Subjected to Normothermic Machine Perfusion. *Biomedicines* **10**, (2022).

43. Smith, A. J., Clutton, R. E., Lilley, E., Hansen, K. E. A. & Brattelid, T. PREPARE: guidelines for planning animal research and testing. *Lab. Anim.* **52**, 135–141 (2018).

44. Dondossola, D. et al. Twelve-hour normothermic liver perfusion in a rat model: characterization of the changes in the ex-situ bio-molecular phenotype and metabolism. *Sci. Rep.* **14**, 1–13 (2024).

45. Meszaros, A. T. et al. Mitochondrial respiration during normothermic liver machine perfusion predicts clinical outcome. *EBioMedicine* **85**, (2022).

46. Pool, M. et al. Infusing mesenchymal stromal cells into porcine kidneys during normothermic machine perfusion: Intact MSCs can be traced and localised to Glomeruli. *Int. J. Mol. Sci.* **20**, 1–15 (2019).

47. Provitera, L. et al. Cyclic nucleotide-dependent relaxation in human umbilical vessels. *J. Physiol. Pharmacol.* **70**, 619–630 (2019).

48. Watson, C. J. E. et al. Observations on the ex situ perfusion of livers for transplantation. *Am. J. Transplant.* **18**, 2005–2020 (2018).

49. Wu, M. Y. et al. Current mechanistic concepts in ischemia and reperfusion injury. *Cell. Physiol. Biochem.* **46**, 1650–1667 (2018).

50. Teodoro, J. S. et al. Shaping of hepatic ischemia/reperfusion events: the crucial role of mitochondria. *Cells* **11**, 1–24 (2022).

51. Soares, R. O. S., Losada, D. M., Jordani, M. C., Évora, P. & Castro-E-Silva, O. Ischemia/reperfusion injury revisited: An overview of the latest pharmacological strategies. *Int. J. Mol. Sci.* **20**, (2019).

52. Schlegel, A. et al. Hypothermic oxygenated perfusion protects from mitochondrial injury before liver transplantation. *EBioMedicine* **60**, (2020).

53. Martin, J. L. et al. Succinate accumulation drives ischaemia-reperfusion injury during organ transplantation. *Nat. Metab.* **1**, 966–974 (2019).

54. Hofmann, J. et al. Restoring mitochondrial function while avoiding redox stress: The key to preventing ischemia/reperfusion injury in machine perfused liver grafts? *Int. J. Mol. Sci.* **21**, (2020).

55. Kron, P., Schlegel, A., Mancina, L., Clavien, P. A. & Dutkowski, P. Hypothermic oxygenated perfusion (HOPE) for fatty liver grafts in rats and humans. *J. Hepatol.* **68**, 82–91 (2018).

56. Peruzzotti-Jametti, L. et al. *Neural stem cells traffic functional mitochondria via extracellular vesicles*. PLoS Biology vol. 19 (2021).

57. Phinney, D. G. et al. Mesenchymal stem cells use extracellular vesicles to outsource mitophagy and shuttle microRNAs. *Nat. Commun.* **6**, 1–15 (2015).

58. Catania, A. et al. The peptide NDP-MSH induces phenotype changes in the heart that resemble ischemic preconditioning. *Peptides* https://doi.org/10.1016/j.peptides.2009.09.030 (2010).

59. Lonati, C. et al. Molecular changes induced in rat liver by hemorrhage and effects of melanocortin treatment. *Anesthesiology* **116**, (2012).

60. Lonati, C. et al. Modulatory effects of NDP-MSH in the regenerating liver after partial hepatectomy in rats. *Peptides* **50**, (2013).

61. Chae, M. S. et al. Serum interleukin-6 and tumor necrosis factor-α are associated with early graft regeneration after living donor liver transplantation. *PLoS One* **13**, 1–13 (2018).

62. Ruan, H. & Dong, L. Q. Adiponectin signaling and function in insulin target tissues. *J. Mol. Cell Biol.* **8**, 101–109 (2016).

63. Blandin, A. et al. Extracellular vesicles are carriers of adiponectin with insulin-sensitizing and anti-inflammatory properties. *Cell Rep.* **42**, (2023).

64. Heydari, M., Cornide-Petronio, M. E., Jiménez-Castro, M. B. & Peralta, C. Data on adiponectin from 2010 to 2020: Therapeutic target and prognostic factor for liver diseases? *Int. J. Mol. Sci.* **21**, 1–24 (2020).

65. Kitto, L. J. & Henderson, N. C. Hepatic Stellate Cell Regulation of Liver Regeneration and Repair. *Hepatol. Commun.* **5**, 358–370 (2021).

66. Hassan, M. N. F. Bin et al. Large-Scale Expansion of Human Mesenchymal Stem Cells. *Stem Cells Int.* **2020**, (2020).

67. du Sert, N. P. et al. The arrive guidelines 2.0: Updated guidelines for reporting animal research. *PLoS Biol.* **18**, 1–12 (2020).

68. Panconesi, R. et al. Mitochondria and ischemia reperfusion injury. *Curr. Opin. Organ Transplant.* **27**, 434–445 (2022).

69. Cillo, U., Nalesso, F. & Bertacco, A. Reply to 'No need for complex blood purification systems for renal replacement therapy during long-term liver normothermic machine perfusion'. Reply to "The importance of developing viability criteria to assess liver grafts undergoing multi- week normothe. *J. Hepatol.* **0**, (2024).

70. Cillo, U., Nalesso, F., Bertacco, A., Indraccolo, S. & Gringeri, E. Normothermic perfusion of a human tumoral liver for 17 days with concomitant extracorporeal blood purification therapy: Case description. *J. Hepatol.* **81**, 96–98 (2024).

71. Eshmuminov, D. et al. An integrated perfusion machine preserves injured human livers for 1 week. *Nat. Biotechnol.* **38**, 189–198 (2020).

72. Lau, N. S. et al. Long-term ex situ normothermic perfusion of human split livers for more than 1 week. *Nat. Commun.* **14**, (2023).

73. Clavien, P. A. et al. Transplantation of a human liver following 3 days of ex situ normothermic preservation. *Nat. Biotechnol.* **40**, 1610–1616 (2022).

74. Lau, N. S. et al. Long-term normothermic perfusion of human livers for longer than 12 days. *Artif. Organs* **46**, 2504–2510 (2022).

75. Bassani, G. A. et al. Ex vivo lung perfusion in the rat: detailed procedure and videos. *PLoS One* **11**, (2016).

76. Lonati, C. et al. NDP-MSH treatment recovers marginal lungs during ex vivo lung perfusion (EVLP). *Peptides* **141**, (2021).

77. Roffia, V. et al. Proteome investigation of rat lungs subjected to Ex vivo perfusion (EVLP). *Molecules* **23**, 1–20 (2018).

78. Balls, M. It's time to reconsider the principles of humane experimental technique. *ATLA Altern. Lab. Anim.* **48**, 40–46 (2020).
79. Russell, W. M. S. & Burch, R. L. The principles of humane experimental technique. *Methuen Co., Ltd.* https://doi.org/10.1017/CBO9781107415324.004 (1959).
80. NC3R. Conducting a pilot study.

Author contributions

U.C. conceptualization, resources, supervision, writing - review & editing; C.L. conceptualization, methodology, investigation, validation, formal analysis, data curation, supervision, resources, project administration, writing – original draft, visualization, writing – review & editing, supervision; A.B. methodology, investigation; data curation, validation, writing – review & editing; L.M. investigation, data curation, formal analysis, visualization, resources, writing – original draft of the supplementary materials, writing – review & editing; M.B. conceptualization, methodology, validation, investigation, data curation, writing – review & editing, project administration; L.B. methodology, investigation, writing – review & editing; F.D. validation, writing – review & editing; D.A.-A. methodology, investigation, writing – review & editing; E.G. validation, writing – review & editing; M.L.B. investigation, validation, writing – review & editing; A.S. validation, writing – review & editing; D.D. conceptualization, methodology, validation, investigation, writing – review & editing, supervision, funding acquisition

Competing interests

The authors declare no competing interests.

Additional information

Supplementary information The online version contains supplementary material available at https://doi.org/10.1038/s41467-024-55217-7.

Correspondence and requests for materials should be addressed to Caterina Lonati.

Peer review information *Nature Communications* thanks Jesus Sierra-Parraga, Michael Nicholson, and the other, anonymous, reviewer(s) for their contribution to the peer review of this work. A peer review file is available.

Reprints and permissions information is available at http://www.nature.com/reprints

Publisher's note Springer Nature remains neutral with regard to jurisdictional claims in published maps and institutional affiliations.

[1]Hepato-Biliary-Pancreatic Surgery and Liver Transplant Unit, General Surgery 2, Department of Surgical, Oncological and Gastroenterological Sciences, University of Padua, Padua, Italy. [2]Center for Preclinical Research, Fondazione IRCCS Ca' Granda Ospedale Maggiore Policlinico, Via Pace 9, 20100 Milan, Italy. [3]School of Cardiovascular and Metabolic Medicine & Sciences, King's College London, London, UK. [4]Division of Transplantation, Department of Surgery, School of Medicine and Public Health, University of Wisconsin, Madison, WI, USA. [5]Department of Veterinary Medical Sciences, University of Bologna, Bologna, Italy. [6]Transplantation Center, Digestive Disease and Surgery Institute, Department of Immunity and Inflammation, Lerner Research Institute, Cleveland Clinic, Cleveland, OH 44106, USA. [7]General and Liver Transplant Surgery Unit, Fondazione IRCCS Ca' Granda Ospedale Maggiore Policlinico, Via Francesco Sforza 35, 20100 Milan, Italy. [8]Department of Pathophysiology and Transplantation, University of Milan, Via Francesco Sforza 35, 20100 Milan, Italy. [10]These authors contributed equally: Umberto Cillo, Caterina Lonati. ✉e-mail: caterina.lonati@gmail.com

Liver NMP Consortium

Domenico Ventrella[5], Camilla Aniballi[5], Margherita Carbonaro[7], Andrea Carlin[8] & Alberto Elmi[5,9]

[9]Department of Veterinary Sciences, University of Pisa, Pisa, Italy.